Engineering Solid Mechanics 8 (2020) 323-336

Contents lists available at GrowingScience

Engineering Solid Mechanics

homepage: www.GrowingScience.com/esm

Improvement on eight-node quadrilateral element (IQ8) using twice-interpolation strategy for linear elastic fracture mechanics

Hoang Lan Ton-That[a*]

[a]*Department of Civil Engineering, Ho Chi Minh City University of Architecture, 196 Pasteur Street, District 3, Ho Chi Minh City, Vietnam*

ARTICLEINFO

Article history:
Received 28 September 2019
Accepted 27 January 2020
Available online
27 January 2020

Keywords:
Twice-interpolation strategy
Eight-node quadrilateral element
Stress intensity factor

ABSTRACT

In this study, an improved eight-node quadrilateral finite element based on a twice-interpolation strategy (TIS) is given for correctly modeling the singular stress field near 2D crack tip of structures. In present approach, the approximation functions for interpolation strategy are established by using the TIS which included nodal values as well as averaged nodal gradients respectively. The stress intensity factors (SIFs) are therefore calculated following the proposed method. The accuracy of the proposed element and its numerical solutions are described by several examples.

1. Introduction

Fracture of structures is of great practical as well as theoretical interest. For example, a large number of important engineering structures, such as pressurized aircraft fuselages, ship hulls, storage tanks and pipelines are carefully designed. Concerns about the safety of such structures have led to a large amount of research related to fracture and fatigue of structural materials. The exact numerical model of the crack-tip field is still a challenge in the scientific community of computational fracture mechanics. Correct predictions of the singular stress fields near the crack tip are necessary in life prediction, maintenance and safety assessment of advanced structures. Many methods such as analytical, semi-analytical, experimental, numerical methods have been presented to fracture modeling over years. On the basis of numerical methods, it is easy to realize that finite element method (FEM) is a powerful tool because of its wide application to solve many technical problems (Anderssohn, Hofmann, & Bahr, 2018; Bathe, 2006; Bui et al., 2016; Gall, Sehitoglu, & Kadioglu, 1996; Hu et al., 2017; Kuna, 2013; Olgierd Cecil Zienkiewicz, Kenneth Morgan, & Morgan, 2006; Olgierd Cecil Zienkiewicz, Robert L Taylor, Perumal Nithiarasu, & Zhu, 1977; Oliva, Cséplö, Materna, & Bláhová, 1997; Trädegård, Nilsson, & Östlund, 1998). Based on singular crack-tip elements or enriched elements (Denda & Marante, 2004; Duan, Lei, & Li, 2011; Fawkes, Owen, & Luxmoore, 1979; Hu et al., 2017; Jayaswal & Grosse, 1993; Kwon & Akin, 1989; Nash Gifford & Hilton, 1978), etc., the FEM can be used for getting the stress intensity factors. Moreover, a smoothing activity used to stresses recovery at the post-processing state is commonly

* Corresponding author.
E-mail addresses: lan.tonthathoang@uah.edu.vn (H. L. Ton-That)

doi: 10.5267/j.esm.2020.3.005

required by the FEM. Thence, several developments of new or improved numerical techniques were introduced to pass the existing difficulties in the classical methods, for example, the extended finite element method (XFEM) (Bergara, Dorado, Martin-Meizoso, & Martínez-Esnaola, 2017; Feng & Li, 2018; Giner, Sukumar, Tarancón, & Fuenmayor, 2009; Moës, Dolbow, & Belytschko, 1999; Wen & Tian, 2016), meshfree methods and coupled FE-EFG method (Kumar, Singh, & Mishra, 2015; Oliveira et al., 2019; Ramalho, Belinha, & Campilho, 2019; Sun, Hu, & Liew, 2007), smoothed FEM (H. Chen, Wang, Liu, Wang, & Sun, 2016; L. Chen, Liu, Jiang, Zeng, & Zhang, 2011; Liu et al., 2012; Nguyen-Van, Ton-That, Chau-Dinh, & Dao, 2018; Nguyen-Xuan, Liu, Nourbakhshnia, & Chen, 2012; That-Hoang, Nguyen-Van, Chau-Dinh, & Huynh-Van, 2018), extended isogeometric analysis (Bhardwaj, Singh, & Mishra, 2013; Bui, 2015a, 2015b; Shojaee & Daneshmand, 2015; Yin, Yu, Bui, Zheng, & Gu, 2019), phantom-node method (Thanh Chau-Dinh, Mai-Van, Zi, & Rabczuk, 2018; T. Chau-Dinh & Zi, 2011; Thanh Chau-Dinh, Zi, Lee, Rabczuk, & Song, 2012), etc. In this paper, we present an improved eight-node quadrilateral finite element based on a twice-interpolation strategy (TIS) with smooth nodal stresses that can pass the difficulties arose in the standard FEM. In addition to the advantages, FEM also exists some disadvantages such as the discontinuity of gradients of field variables among internal element edges or at nodes. In practice, the post-processing procedure is usually required to get the smoothing operation to the nodal stress. In recent years, some authors (Zheng et al., 2010) presented an improved triangular element for elastostatic problems related to the new concept TIS of the interpolation functions. Their element with various desirable features such as the continuous nodal stress and the higher accuracy of the solutions are not available in the standard elements. The main idea of the TIS is based on the approximation functions that control not only the nodal values but also the averaged nodal gradients as interpolation conditions, see (Zheng et al., 2010) for details. Nevertheless, the major motivation of applying the TIS is to formulate the trial solution as well as its derivatives continuous across inter-element boundaries. The stress by using this strategy can be smoothed over each domain of element to improve the accuracy of solution without the post-processing process. Another important issue should be noted that the TIS does not change the total number of degrees of freedom (DOFs) of the whole system. The TIS is also applied and extended in some references (Bui et al., 2014; Ton-That, Nguyen-Van, & Chau-Dinh, 2019; Ton That, Nguyen-Van, & Chau-Dinh, 2020), respectively.

The main objective of this paper is to improve the eight-node quadrilateral finite element based on TIS for correctly modeling singular stress fields near 2D crack tips of structures. The stress intensity factors (SIFs) calculated by the proposed element are validated against reference solutions. The body of the report is organized into five Sections. In section 2, formulation of this new element (IQ8) for 2D cracks in elastic structures is presented in which the construction of the shape functions and their properties are recommended. The little modification of IQ8 become singular IQ8 around crack tip and the SIFs values are determined in section 3. Several examples are subsequently presented in section 4.

2. Formulation of IQ8 element for linear elastic fracture mechanics

In this section, the construction of the IQ8 shape functions and their properties are briefly given. A point **x** (x, y) is in a eight-node quadrilateral element with eight nodes *i, j, k, m, n, p, q* and *r* as schematically sketched in Fig.1a. We here denote by S_{inr}, S_{jpn}, S_{kqp} and S_{mrq} elements that share nodes *i, j, k, m, n, p, q* and *r*, respectively. All nodes of elements S_{inr}, S_{jpn}, S_{kqp} and S_{mrq} are called the supporting nodes of the point **x** in the IQ8 element. This leads to the support domain for point **x** of IQ8 being larger than the support domain of standard FEM. The trial solution at point **x** is therefore given as

$$u^h(x) = \sum_{l=1}^{n_{sp}} \tilde{N}_l(\mathbf{x}) d_l = \tilde{\mathbf{N}}(\mathbf{x})\mathbf{d} \tag{1}$$

In Eq. (1), the twice-interpolation shape function $\tilde{N}_l$ is recommended

$$\tilde{N}_l = \underbrace{\phi_i N_l^{[i]} + \phi_{ix}\bar{N}_{l,x}^{[i]} + \phi_{iy}\bar{N}_{l,y}^{[i]}}_{\text{node } i} + \underbrace{\phi_j N_l^{[j]} + \phi_{jx}\bar{N}_{l,x}^{[j]} + \phi_{jy}\bar{N}_{l,y}^{[j]}}_{\text{node } j} + \underbrace{\phi_k N_l^{[k]} + \phi_{kx}\bar{N}_{l,x}^{[k]} + \phi_{ky}\bar{N}_{l,y}^{[k]}}_{\text{node } k} + \underbrace{\phi_m N_l^{[m]} + \phi_{mx}\bar{N}_{l,x}^{[m]} + \phi_{my}\bar{N}_{l,y}^{[m]}}_{\text{node } m}$$
$$+ \underbrace{\phi_n N_l^{[n]} + \phi_{nx}\bar{N}_{l,x}^{[n]} + \phi_{ny}\bar{N}_{l,y}^{[n]}}_{\text{node } n} + \underbrace{\phi_p N_l^{[p]} + \phi_{px}\bar{N}_{l,x}^{[p]} + \phi_{py}\bar{N}_{l,y}^{[p]}}_{\text{node } p} + \underbrace{\phi_q N_l^{[q]} + \phi_{qx}\bar{N}_{l,x}^{[q]} + \phi_{qy}\bar{N}_{l,y}^{[q]}}_{\text{node } q} + \underbrace{\phi_r N_l^{[r]} + \phi_{rx}\bar{N}_{l,x}^{[r]} + \phi_{ry}\bar{N}_{l,y}^{[r]}}_{\text{node } r} \quad (2)$$

in which d_f and $N_f^{[i]}$ are called the nodal displacement vector and the shape function related to node i. Moreover, n_{sp} is also called the total number of the supporting nodes due to the point **x**. The formulation of the average derivative of the shape functions at node i is presented as below and the same is built for other nodes.

$$\bar{N}_{l,x}^{[i]} = \sum_{e\in S_{inr}} \left(\omega_e N_{l,x}^{[i][e]}\right);\ \bar{N}_{l,y}^{[i]} = \sum_{e\in S_{inr}} \left(\omega_e N_{l,y}^{[i][e]}\right) \quad (3)$$

In Eq. (3), the term $N_{l,x}^{[i][e]}$ is the derivative of $N_l^{[i]}$ calculated in element e, and ω_e is called the weight function of element $e \in S_{inr}$, which is defined by

$$\omega_e = \frac{\Delta_e}{\sum_{\bar{e}\in S_{inr}} \Delta_{\bar{e}}} \text{ with } e \in S_{inr} \quad (4)$$

with Δ_e being the area of the element e. In Eq. (2), the functions ϕ_i, ϕ_{ix} and ϕ_{iy} calling the polynomial related to node i must be content with the conditions (see Appendix for proving them)

$$\phi_i(\mathbf{x}_l) = \delta_{il},\ \phi_{i,x}(\mathbf{x}_l) = 0,\ \phi_{i,y}(\mathbf{x}_l) = 0,\ \phi_{ix}(\mathbf{x}_l) = 0,\ \phi_{ix,x}(\mathbf{x}_l) = \delta_{il},\ \phi_{ix,y}(\mathbf{x}_l) = 0$$
$$\phi_{iy}(\mathbf{x}_l) = 0,\ \phi_{iy,x}(\mathbf{x}_l) = 0,\ \phi_{iy,y}(\mathbf{x}_l) = \delta_{il} \quad (5)$$

in which l is from the indices i, j, k, m, n, p, q and r, and

$$\delta_{il} = \begin{cases} 1 & if \quad i = l \\ 0 & if \quad i \neq l \end{cases} \quad (6)$$

Note that the above conditions have to be twirled in a similar way to different functions, i.e., ϕ_j, ϕ_{jx}, ϕ_{jy}, ϕ_k, ϕ_{kx}, ϕ_{ky}, ϕ_m, ϕ_{mx}, ϕ_{my}, ϕ_n, ϕ_{nx}, ϕ_{ny}, ϕ_p, ϕ_{px}, ϕ_{py}, ϕ_q, ϕ_{qx}, ϕ_{qy}, ϕ_r, ϕ_{rx}, and ϕ_{ry}. These polynomial basis functions ϕ_i, ϕ_{ix} and ϕ_{iy} for the IQ8 element are given by (7)

$$\begin{aligned}
\phi_i &= L_i + L_i^2 L_j + L_i^2 L_k + L_i^2 L_m + L_i^2 L_n + L_i^2 L_p + L_i^2 L_q + L_i^2 L_r \\
&\quad - L_i L_j^2 - L_i L_k^2 - L_i L_m^2 - L_i L_n^2 - L_i L_p^2 - L_i L_q^2 - L_i L_r^2 \\
\phi_{ix} &= -(x_i - x_j)\left(L_i^2 L_j + 0.5L_i L_j L_k + 0.5L_i L_j L_m + 0.5L_i L_j L_n + 0.5L_i L_j L_p + 0.5L_i L_j L_q + 0.5L_i L_j L_r\right) \\
&\quad -(x_i - x_k)\left(L_i^2 L_k + 0.5L_i L_k L_j + 0.5L_i L_k L_m + 0.5L_i L_k L_n + 0.5L_i L_k L_p + 0.5L_i L_k L_q + 0.5L_i L_k L_r\right) \\
&\quad -(x_i - x_m)\left(L_i^2 L_m + 0.5L_i L_m L_j + 0.5L_i L_m L_k + 0.5L_i L_m L_n + 0.5L_i L_m L_p + 0.5L_i L_m L_q + 0.5L_i L_m L_r\right) \\
&\quad -(x_i - x_n)\left(L_i^2 L_n + 0.5L_i L_n L_j + 0.5L_i L_n L_k + 0.5L_i L_n L_m + 0.5L_i L_n L_p + 0.5L_i L_n L_q + 0.5L_i L_n L_r\right) \\
&\quad -(x_i - x_p)\left(L_i^2 L_p + 0.5L_i L_p L_j + 0.5L_i L_p L_k + 0.5L_i L_p L_m + 0.5L_i L_p L_n + 0.5L_i L_p L_q + 0.5L_i L_p L_r\right) \\
&\quad -(x_i - x_q)\left(L_i^2 L_q + 0.5L_i L_q L_j + 0.5L_i L_q L_k + 0.5L_i L_q L_m + 0.5L_i L_q L_n + 0.5L_i L_q L_p + 0.5L_i L_q L_r\right) \\
&\quad -(x_i - x_r)\left(L_i^2 L_r + 0.5L_i L_r L_j + 0.5L_i L_r L_k + 0.5L_i L_r L_m + 0.5L_i L_r L_n + 0.5L_i L_r L_p + 0.5L_i L_r L_q\right) \\
\phi_{iy} &= -(y_i - y_j)\left(L_i^2 L_j + 0.5L_i L_j L_k + 0.5L_i L_j L_m + 0.5L_i L_j L_n + 0.5L_i L_j L_p + 0.5L_i L_j L_q + 0.5L_i L_j L_r\right) \\
&\quad -(y_i - y_k)\left(L_i^2 L_k + 0.5L_i L_k L_j + 0.5L_i L_k L_m + 0.5L_i L_k L_n + 0.5L_i L_k L_p + 0.5L_i L_k L_q + 0.5L_i L_k L_r\right) \\
&\quad -(y_i - y_m)\left(L_i^2 L_m + 0.5L_i L_m L_j + 0.5L_i L_m L_k + 0.5L_i L_m L_n + 0.5L_i L_m L_p + 0.5L_i L_m L_q + 0.5L_i L_m L_r\right) \\
&\quad -(y_i - y_n)\left(L_i^2 L_n + 0.5L_i L_n L_j + 0.5L_i L_n L_k + 0.5L_i L_n L_m + 0.5L_i L_n L_p + 0.5L_i L_n L_q + 0.5L_i L_n L_r\right) \\
&\quad -(y_i - y_p)\left(L_i^2 L_p + 0.5L_i L_p L_j + 0.5L_i L_p L_k + 0.5L_i L_p L_m + 0.5L_i L_p L_n + 0.5L_i L_p L_q + 0.5L_i L_p L_r\right) \\
&\quad -(y_i - y_q)\left(L_i^2 L_q + 0.5L_i L_q L_j + 0.5L_i L_q L_k + 0.5L_i L_q L_m + 0.5L_i L_q L_n + 0.5L_i L_q L_p + 0.5L_i L_q L_r\right) \\
&\quad -(y_i - y_r)\left(L_i^2 L_r + 0.5L_i L_r L_j + 0.5L_i L_r L_k + 0.5L_i L_r L_m + 0.5L_i L_r L_n + 0.5L_i L_r L_p + 0.5L_i L_r L_q\right)
\end{aligned} \quad (7)$$

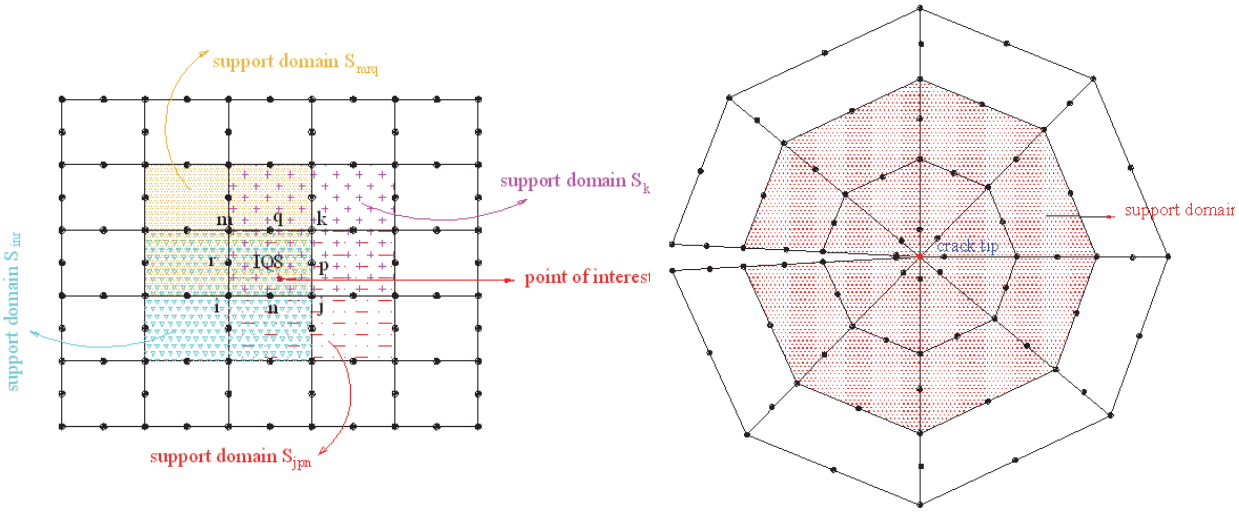

(a) (b)

Fig. 1. (a) Eight-node quadrilateral element in 2D with twice-interpolation strategy and its support domain, (b) Illustration of the support domains around crack tip.

In Eq. (7), other functions can be also presented in the same way by a circular substitution of indices *i, j, k, m, n, p, q* and *r*. In addition, L_i, L_j, L_k, L_m, L_n, L_p, L_q, and L_r are called the area coordinates of the point **x** in the eight-node quadrilateral element *i, j, k, m, n, p, q, r* see (Zheng et al., 2010) for more details. It is very important to see these shape functions are sufficient polynomials, hold Kronecker's delta function property and satisfy properties of the partition of unity. The element stiffness matrix $\mathbf{K_e}$ can be finally expressed as

$$\mathbf{K}_e = \int_{\Omega_e} \tilde{\mathbf{B}}_e^T \mathbf{D} \tilde{\mathbf{B}}_e d\Omega \tag{8}$$

with **D** is elastic tensor and

$$\tilde{\mathbf{B}}_e = \begin{bmatrix} \tilde{N}_{1,x} & 0 & \tilde{N}_{2,x} & 0 & \dots & \tilde{N}_{l,x} & 0 & \dots & \tilde{N}_{n_{sp},x} & 0 \\ 0 & \tilde{N}_{1,y} & 0 & \tilde{N}_{2,y} & \dots & 0 & \tilde{N}_{l,y} & \dots & 0 & \tilde{N}_{n_{sp},y} \\ \tilde{N}_{1,y} & \tilde{N}_{1,x} & \tilde{N}_{2,y} & \tilde{N}_{2,x} & \dots & \tilde{N}_{l,y} & \tilde{N}_{l,x} & \dots & \tilde{N}_{n_{sp},y} & \tilde{N}_{n_{sp},x} \end{bmatrix}_{3\times 2n_{sp}} \tag{9}$$

n_{sp} is recalled the total number of the supporting nodes due to the point **x**.

3. Modified IQ8 element around crack tip

For a long time, finite element analyses have been excellent tools for utilization in the evaluation of cracking in structures. In the mid 1970s, (Barsoum, 1974), (Henshell & Shaw, 1975) independently discovered that by taking the mid-side nodes of an element that are adjacent to the tip of crack and moving them to the quarter-point of the element side, the singular stress field which occurs at the tip of crack could be created. It was a meaningful discovery since researchers had spent goodly efforts trying to develop special elements which could capture this behavior. While some of these special elements have achieved some success, implementing these elements into general purpose finite element codes was not practical. The fact that the quarter-point element (QPE) may be used in any finite element code makes it highly valuable.

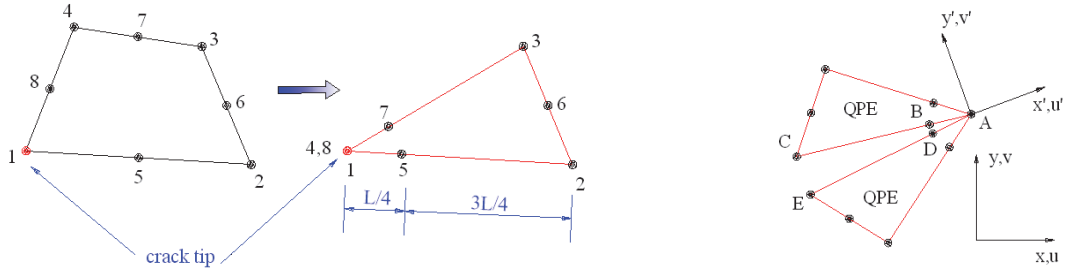

(a) (b)

Fig. 2. Eight-node quadrilateral element: (a) with quarter-point nodes, (b) nodal lettering for stress intensity computation.

In this paper, we use quarter-point techniques to modify eight-node quadrilateral element as show in Fig.2a if node 1 is considered as crack tip point. The support domains around crack tip are also presented in Fig.1b, respectively. The SIFs are directly evaluated from

$$\mathrm{K_I} = \frac{G}{K+1}\sqrt{\left(\frac{2\pi}{L}\right)\left\{4\left(v_B^{'}-v_D^{'}\right)-\left(v_C^{'}-v_E^{'}\right)\right\}}$$
$$\mathrm{K_{II}} = \frac{G}{K+1}\sqrt{\left(\frac{2\pi}{L}\right)\left\{4\left(u_B^{'}-u_D^{'}\right)-\left(u_C^{'}-u_E^{'}\right)\right\}} \tag{10}$$

where G is shear modulus, K is *3-4v* for plane strain and *(3-v)/(1+v)* for plane stress, L is QPE length along crack face, and *u', v'* are local displacement along and normal to crack face as depicted in Fig.2b.

4. Numerical solutions

In this section, we will examine and assess the IQ8 element through numerical examples.

4.1 An edge crack under tensile load

Firstly, a finite rectangular plate with an edge crack subjected to a uniform tensile load on the top of it is given. The geometry of this test specimen is schematically depicted in Fig.3a. The bottom edge of the specimen is fully clamped. The dimensionless geometric parameters for this specimen is L = 16 for the length of the specimen, W = 7 for the width, and $a = W/2$ for crack length, respectively.

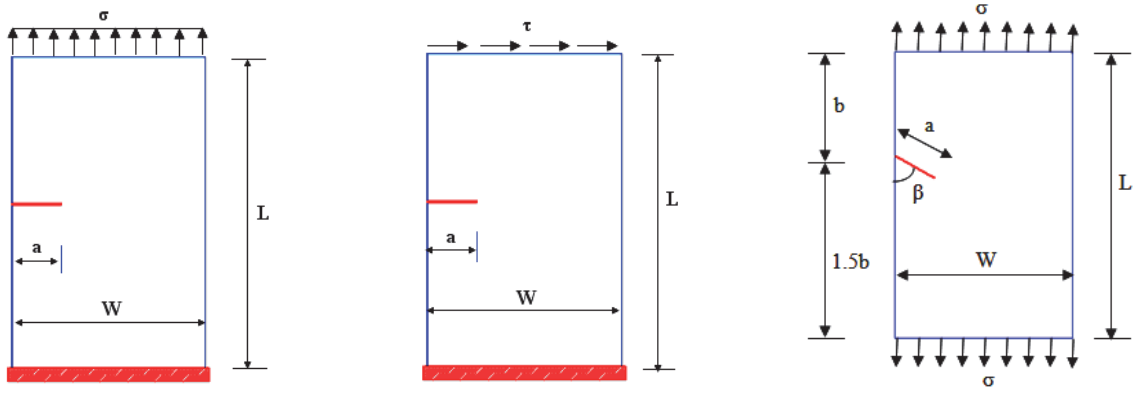

(a) (b) (c)

Fig. 3. Geometric notation of an edge crack under (a) tensile load, (b) shear load and (c) slant edge crack plate under tension.

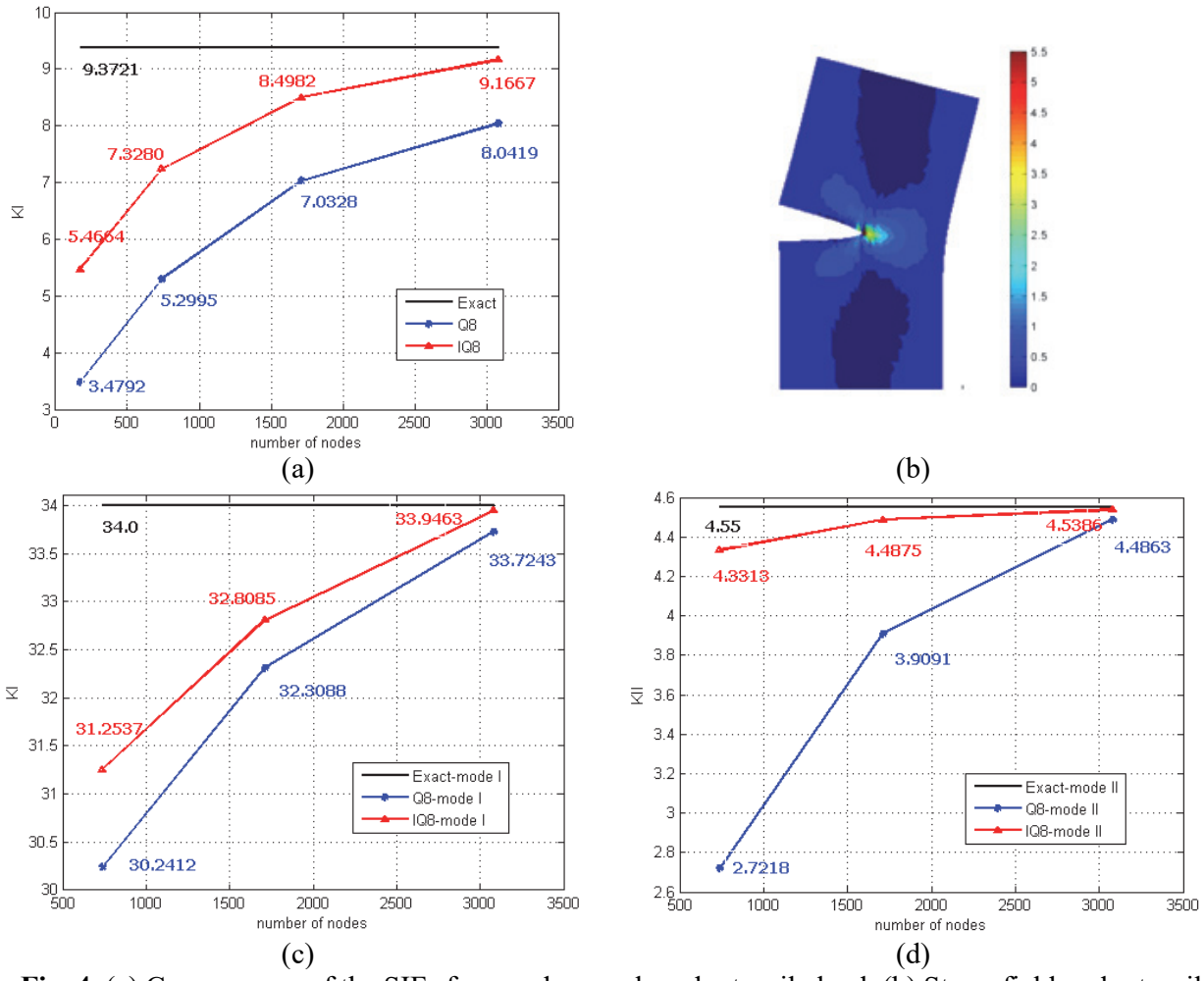

Fig. 4. (a) Convergence of the SIFs for an edge crack under tensile load, (b) Stress field under tensile load, (c) Convergence of the SIFs (KI) for an edge crack under shear load, (d) Convergence of the SIFs (KII) for an edge crack under shear load.

The value $\sigma = 1$ is assigned to the top of the plate, and only mode I can be considered. The numerical mode-I SIF is validated with the analytical solutions given by (Ewalds & Wanhill, 1989) $K_I = C\sigma\sqrt{\pi a}$, where C is determined by

$$C = 1.12 - 0.231\left(\frac{a}{W}\right) + 10.55\left(\frac{a}{W}\right)^2 - 21.72\left(\frac{a}{W}\right)^3 + 30.39\left(\frac{a}{W}\right)^4 \quad (11)$$

The computed results and the convergence of mode-I SIF are thus presented in Fig. 4a, which indicates higher accuracy of the mode-I SIF gained by the IQ8 than the conventional Q8 when increasing the number of elements. To exhibit the performance of IQ8 in stress distribution, we plot the σ_x stress contour which is shown in Fig.4b.

4.2. An edge crack under shear load

By changing from uniform tensile load to uniform shear load on the top of the plate, we have the next example. The geometry of this test specimen is also schematically depicted in Fig.3b. The bottom edge of the specimen is fully clamped. The dimensionless geometric parameter for this specimen is repeated as follows: $L = 16$ for the length of the specimen, $W = 7$ for the width, and $a = W/2$ for crack length. The value $\tau = 1$ is assigned to the top of the plate. This is a mixed mode problem and the exact solutions are $K_I = 34.0$ and $K_{II} = 4.55$ for this case (Moës et al., 1999). Once again, the computer results are presented in Fig. 4c & d, which shows higher accuracy than the conventional Q8 when increasing the number of elements.

4.3 A slant edge crack plate under tension

A rectangular plate is shown in Fig.3c with the dimensions of L = 2.5 cm and $b = W$ = 1.0 cm. An oblique edge crack of length a is in plate with β = 67.5°. Material properties of the plate are: E = 190GPa, ν = 0.25. The stress intensity factors of the crack tip K_I and K_{II} are calculated with the strategic mesh by MATLAB code as shown in Fig.5a while the plate is subjected to uniform tension on the ends. The analytical solution of this model is given as

$$K_I = F_I\sigma\sqrt{\pi a} \qquad K_{II} = F_{II}\sigma\sqrt{\pi a} \qquad \Rightarrow \qquad F_i = \frac{K_i}{\sigma\sqrt{\pi a}} \qquad \text{with} \qquad i = I, II \tag{11}$$

Fig.5b show the normalized stress intensity factors (F_I, F_{II}) and the comparison with the results by (Aliabadi et al., 1989) who used the boundary element method to perform similar studies on the same problem. The results are in good agreement.

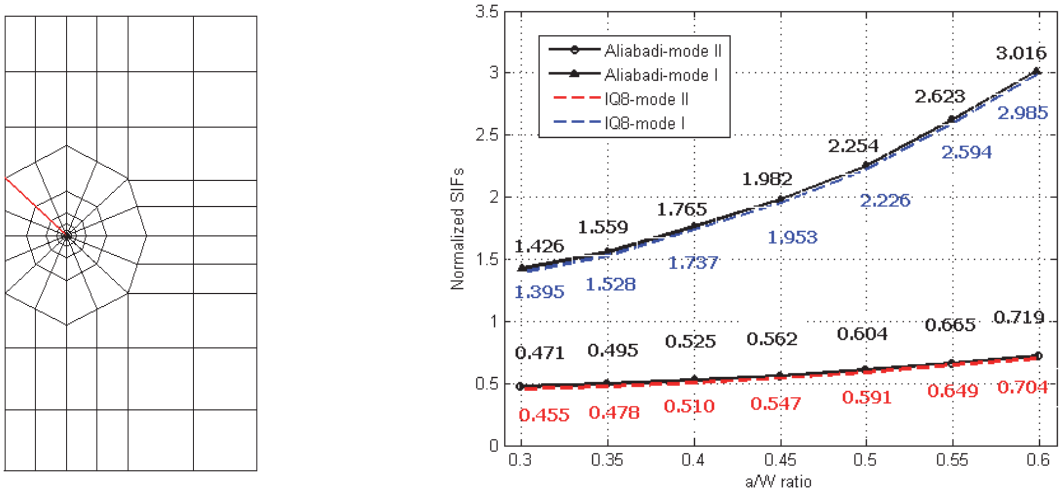

(a) (b)

Fig. 5. (a) The strategic mesh, (b) Normalized SIFs (F_I, F_{II}).

4.4 A three-point bending beam with one edge crack

Finally, let us consider a three-point bending beam with one edge crack and the strategic mesh as depicted in Figs.6 and 7a. The geometric parameters of this structure are W = 6, L = 12 and a = 0.3W. The structure is also subjected to a concentrated force F = 1 and the edge crack is located at the mid-span of its, as the trend of only developing mode I-crack.

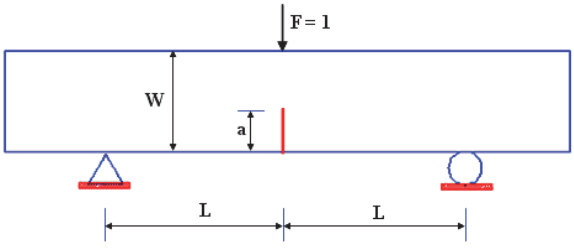

Fig. 6. Geometric notation of a three-point bending beam.

The analytical solution with crack length a = 0.3W is given by (Kang et al. 2015; Srawley, 1976). Additionally, higher value of the SIFs computed based on the PUM (Wu & Cai, 2014) over the analytical results can be observed in this reference. The calculated mode-I SIF of this structure based on the IQ8 are compared with the PUM and the analytical method as in Fig.7b with good convergence for the IQ8, respectively.

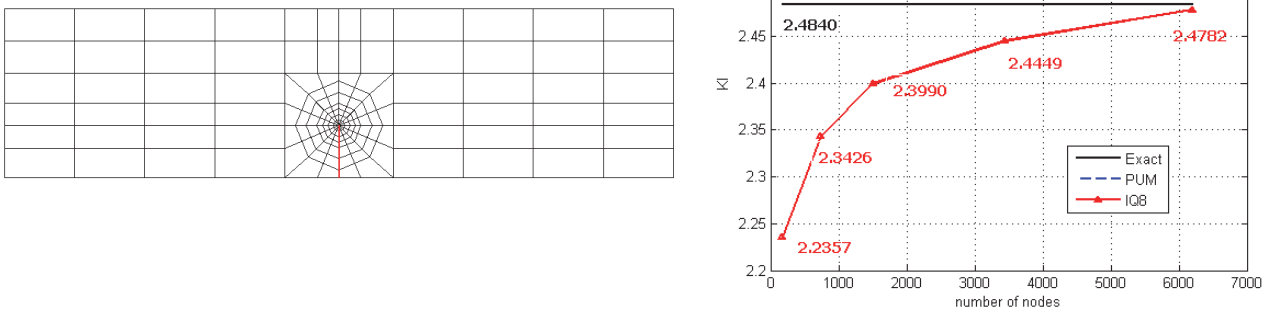

(a) (b)

Fig. 7. (a) The strategic mesh, (b) Mode-I SIF of a three-point bending beam with an edge crack.

5. Conclusions

An accurate numerical method based on the IQ8 element is firstly developed for correctly modeling 2D cracks in structures. We have used the IQ8 element to analyze the SIFs of some linear elastic fracture mechanics problems in 2D, respectively. In each case of the study with different load, the SIFs are calculated, and they have been found to agree well with the other analytical results, or with the other numerical methods. Based on the IQ8 element, the present numerical solutions offer higher accuracy than others of the common element. And the applicability of IQ8 element has been clearly shown as above section. The better numerical solutions and the smoother distributions of stresses around the crack tip which are not achieved by the standard elements will be provided when using the IQ8 elements. The computational time of the new IQ8 element was not included in present paper. In fact, this computational time is higher than that based on the standard element because of the TIS procedure, but one will not need a post-processing of any smoothing operation.

References

Aliabadi, M. H., Cartwright, D. J., & Rooke, D. P. (1989). Fracture-mechanics weight-functions by the removal of singular fields using boundary element analysis. *International Journal of Fracture, 40*(4), 271-284.

Anderssohn, R., Hofmann, M., & Bahr, H. A. (2018). FEM-bifurcation analysis for 3D crack patterns. *Engineering Fracture Mechanics, 202*, 363-374.

Barsoum, R. S. (1974). Application of quadratic isoparametric finite elements in linear fracture mechanics. *International Journal of Fracture, 10*(4), 603-605.

Bathe, K.-J. (2006). *Finite element procedures*. USA: Prentice Hall, Pearson Education, Inc.

Bergara, A., Dorado, J. I., Martin-Meizoso, A., & Martínez-Esnaola, J. M. (2017). Fatigue crack propagation in complex stress fields: Experiments and numerical simulations using the Extended Finite Element Method (XFEM). *International Journal of Fatigue, 103*, 112-121.

Bhardwaj, G., Singh, I. V., & Mishra, B. K. (2013). Numerical Simulation of Plane Crack Problems Using Extended Isogeometric Analysis. *Procedia Engineering, 64*, 661-670.

Bui, T. Q. (2015a). Extended isogeometric dynamic and static fracture analysis for cracks in piezoelectric materials using NURBS. *Computer Methods in Applied Mechanics and Engineering, 295*(Supplement C), 470-509.

Bui, T. Q. (2015b). Extended isogeometric dynamic and static fracture analysis for cracks in piezoelectric materials using NURBS. *Computer Methods in Applied Mechanics and Engineering, 295*, 470-

509.

Bui, T. Q., Do, T. V., Ton, L. H. T., Doan, D. H., Tanaka, S., Pham, D. T., . . . Hirose, S. (2016). On the high temperature mechanical behaviors analysis of heated functionally graded plates using FEM and a new third-order shear deformation plate theory. *Composites Part B: Engineering, 92*, 218-241.

Bui, T. Q., Vo, D. Q., Zhang, C., & Nguyen, D. D. (2014). A consecutive-interpolation quadrilateral element (CQ4): Formulation and applications. *Finite Elements in Analysis and Design, 84*, 14-31.

Chau-Dinh, T., Mai-Van, C., Zi, G., & Rabczuk, T. (2018). New kinematical constraints of cracked MITC4 shell elements based on the phantom-node method for fracture analysis. *Engineering Fracture Mechanics, 199*, 159-178.

Chau-Dinh, T., & Zi, G. (2011). A Phantom-Node Method for Predicting Residual Strength in Shell Structures with a Single Crack Based on a Crack Tip Opening Angle Criterion. *Procedia Engineering, 14*, 630-635.

Chau-Dinh, T., Zi, G., Lee, P.-S., Rabczuk, T., & Song, J.-H. (2012). Phantom-node method for shell models with arbitrary cracks. *Computers & Structures, 92-93*, 242-256.

Chen, H., Wang, Q., Liu, G. R., Wang, Y., & Sun, J. (2016). Simulation of thermoelastic crack problems using singular edge-based smoothed finite element method. *International Journal of Mechanical Sciences, 115-116*, 123-134.

Chen, L., Liu, G. R., Jiang, Y., Zeng, K., & Zhang, J. (2011). A singular edge-based smoothed finite element method (ES-FEM) for crack analyses in anisotropic media. *Engineering Fracture Mechanics, 78*(1), 85-109.

Denda, M., & Marante, M. E. (2004). Mixed mode BEM analysis of multiple curvilinear cracks in the general anisotropic solids by the crack tip singular element. *International Journal of Solids and Structures, 41*(5), 1473-1489.

Duan, J. B., Lei, Y. J., & Li, D. K. (2011). Fracture analysis of linear viscoelastic materials using triangular enriched crack tip elements. *Finite Elements in Analysis and Design, 47*(10), 1157-1168.

Ewalds, H., & Wanhill, R. (1989). *Fracture Mechanics*. New York: Edward Arnold.

Fawkes, A. J., Owen, D. R. J., & Luxmoore, A. R. (1979). An assessment of crack tip singularity models for use with isoparametric elements. *Engineering Fracture Mechanics, 11*(1), 143-159.

Feng, S. Z., & Li, W. (2018). An accurate and efficient algorithm for the simulation of fatigue crack growth based on XFEM and combined approximations. *Applied Mathematical Modelling, 55*, 600-615.

Gall, K., Sehitoglu, H., & Kadioglu, Y. (1996). FEM study of fatigue crack closure under double slip. *Acta Materialia, 44*(10), 3955-3965.

Giner, E., Sukumar, N., Tarancón, J. E., & Fuenmayor, F. J. (2009). An Abaqus implementation of the extended finite element method. *Engineering Fracture Mechanics, 76*(3), 347-368.

Henshell, R. D., & Shaw, K. G. (1975). Crack tip finite elements are unnecessary. *International Journal for Numerical Methods in Engineering, 9*(3), 495-507.

Hu, X., Bui, T. Q., Wang, J., Yao, W., Ton, L. H. T., Singh, I. V., & Tanaka, S. (2017). A new cohesive crack tip symplectic analytical singular element involving plastic zone length for fatigue crack growth prediction under variable amplitude cyclic loading. *European Journal of Mechanics - A/Solids, 65*, 79-90.

Jayaswal, K., & Grosse, I. R. (1993). Finite element error estimation for crack tip singular elements. *Finite Elements in Analysis and Design, 14*(1), 17-35.

Kang, Z., Bui, T. Q., Nguyen, D. D., Saitoh, T., & Hirose, S. (2015). An extended consecutive-interpolation quadrilateral element (XCQ4) applied to linear elastic fracture mechanics. *Acta Mechanica, 226*(12), 3991-4015.

Kumar, S., Singh, I. V., & Mishra, B. K. (2015). A homogenized XFEM approach to simulate fatigue crack growth problems. *Computers & Structures, 150*(Supplement C), 1-22.

Kuna, M. (2013). *Finite Elements in Fracture Mechanics: Theory - Numerics - Applications*: Springer

Science & Business Media.
Kwon, Y. W., & Akin, J. E. (1989). Development of a derivative singular element for application to crack propagation problems. *Computers & Structures, 31*(3), 467-471.
Liu, P., Bui, T. Q., Zhang, C., Yu, T. T., Liu, G. R., & Golub, M. V. (2012). The singular edge-based smoothed finite element method for stationary dynamic crack problems in 2D elastic solids. *Computer Methods in Applied Mechanics and Engineering, 233-236*(Supplement C), 68-80.
Moës, N., Dolbow, J., & Belytschko, T. (1999). A finite element method for crack growth without remeshing. *International Journal for Numerical Methods in Engineering, 46*(1), 131-150.
Nash Gifford, L., & Hilton, P. D. (1978). Stress intensity factors by enriched finite elements. *Engineering Fracture Mechanics, 10*(3), 485-496.
Nguyen-Van, H., Ton-That, H. L., Chau-Dinh, T., & Dao, N. D. (2018). *Nonlinear Static Bending Analysis of Functionally Graded Plates Using MISQ24 Elements with Drilling Rotations.* Paper presented at the Proceedings of the International Conference on Advances in Computational Mechanics 2017, Singapore.
Nguyen-Xuan, H., Liu, G. R., Nourbakhshnia, N., & Chen, L. (2012). A novel singular ES-FEM for crack growth simulation. *Engineering Fracture Mechanics, 84*, 41-66.
Olgierd Cecil Zienkiewicz, Kenneth Morgan, & Morgan, K. (2006). *Finite elements and approximation*: Courier Corporation.
Olgierd Cecil Zienkiewicz, Robert L Taylor, Perumal Nithiarasu, & Zhu, J. (1977). *The finite element method*: McGraw-hill.
Oliva, V., Cséplö, L., Materna, A., & Bláhová, L. (1997). FEM simulation of fatigue crack growth. *Materials Science and Engineering: A, 234-236*, 517-520.
Oliveira, T., Vélez, W., Santana, E., Araújo, T., Mendonça, F., & Portela, A. (2019). A local mesh free method for linear elasticity and fracture mechanics. *Engineering Analysis with Boundary Elements, 101*, 221-242.
Ramalho, L. D. C., Belinha, J., & Campilho, R. D. S. G. (2019). The numerical simulation of crack propagation using radial point interpolation meshless methods. *Engineering Analysis with Boundary Elements, 109*, 187-198.
Shojaee, S., & Daneshmand, A. (2015). Crack analysis in media with orthotropic Functionally Graded Materials using extended Isogeometric analysis. *Engineering Fracture Mechanics, 147*, 203-227.
Srawley, J. E. (1976). Wide range stress intensity factor expressions for ASTM E 399 standard fracture toughness specimens. *International Journal of Fracture, 12*(3), 475-476.
Sun, Y., Hu, Y. G., & Liew, K. M. (2007). A mesh-free simulation of cracking and failure using the cohesive segments method. *International Journal of Engineering Science, 45*(2), 541-553.
That-Hoang, L. T., Nguyen-Van, H., Chau-Dinh, T., & Huynh-Van, C. (2018). Enhancement to four-node quadrilateral plate elements by using cell-based smoothed strains and higher-order shear deformation theory for nonlinear analysis of composite structures. *Journal of Sandwich Structures & Materials*, 1099636218797982.
Ton-That, H. L., Nguyen-Van, H., & Chau-Dinh, T. (2019). An Improved Four-Node Element for Analysis of Composite Plate/Shell Structures Based on Twice Interpolation Strategy. *International Journal of Computational Methods*, 1950020.
Ton That, H. L., Nguyen-Van, H., & Chau-Dinh, T. (2020). Nonlinear Bending Analysis of Functionally Graded Plates Using SQ4T Elements based on Twice Interpolation Strategy. *Journal of Applied and Computational Mechanics, 6*(1), 125-136.
Trädegård, A., Nilsson, F., & Östlund, S. (1998). FEM-remeshing technique applied to crack growth problems. *Computer Methods in Applied Mechanics and Engineering, 160*(1), 115-131.
Wen, L., & Tian, R. (2016). Improved XFEM: Accurate and robust dynamic crack growth simulation. *Computer Methods in Applied Mechanics and Engineering, 308*, 256-285.
Wu, J., & Cai, Y. (2014). A partition of unity formulation referring to the NMM for multiple intersecting crack analysis. *Theoretical and Applied Fracture Mechanics, 72*, 28-36.
Yin, S., Yu, T., Bui, T. Q., Zheng, X., & Gu, S. (2019). Static and dynamic fracture analysis in elastic solids using a multiscale extended isogeometric analysis. *Engineering Fracture Mechanics, 207*,

109-130.

Zheng, C., Wu, S. C., Tang, X. H., & Zhang, J. H. (2010). A novel twice-interpolation finite element method for solid mechanics problems. *Acta Mechanica Sinica, 26*(2), 265-278.

Appendix

Let us consider a quadrilateral element with eight-node as sketched in Fig.1. The functions L_i, L_j, L_k, L_m, L_n, L_p, L_q and L_r are given

$$L_i=-\frac{1}{4}(1-\xi)(1-\eta)(1+\xi+\eta)\ ;\ L_j=-\frac{1}{4}(1+\xi)(1-\eta)(1-\xi+\eta)\ ;\ L_k=-\frac{1}{4}(1+\xi)(1+\eta)(1-\xi-\eta)\ ;\ L_m=-\frac{1}{4}(1-\xi)(1+\eta)(1+\xi-\eta)$$

$$L_n=\frac{1}{2}(1-\xi)(1+\xi)(1-\eta)\ ;\ L_p=\frac{1}{2}(1+\xi)(1+\eta)(1-\eta)\ ;\ L_q=\frac{1}{2}(1-\xi)(1+\xi)(1+\eta)\ ;\ L_r=\frac{1}{2}(1-\xi)(1+\eta)(1-\eta)$$

The derivatives of above functions are

$$\begin{Bmatrix}\frac{\partial}{\partial\xi}\\ \frac{\partial}{\partial\eta}\end{Bmatrix}\begin{bmatrix}L_i & L_j & L_k & L_m & L_n & L_p & L_q & L_r\end{bmatrix}=$$

$$=\begin{bmatrix}-\frac{1}{4}(-1+\eta)(2\xi+\eta) & \frac{1}{4}(-1+\eta)(\eta-2\xi) & \frac{1}{4}(1+\eta)(2\xi+\eta) & -\frac{1}{4}(1+\eta)(\eta-2\xi) & \xi(-1+\eta) & -\frac{1}{2}(1+\eta)(-1+\eta) & -\xi(1+\eta) & \frac{1}{2}(1+\eta)(-\\ -\frac{1}{4}(-1+\xi)(\xi+2\eta) & \frac{1}{4}(1+\xi)(2\eta-\xi) & \frac{1}{4}(1+\xi)(\xi+2\eta) & -\frac{1}{4}(-1+\xi)(2\eta-\xi) & \frac{1}{2}(1+\xi)(-1+\xi) & -\eta(1+\xi) & -\frac{1}{2}(1+\xi)(-1+\xi) & \eta(-1+\end{bmatrix}$$

The Jacobian matrix and its inverse are explicitly expressed as

$$\mathbf{J}=$$

$$=\begin{bmatrix}-\frac{1}{4}(-1+\eta)(2\xi+\eta) & \frac{1}{4}(-1+\eta)(\eta-2\xi) & \frac{1}{4}(1+\eta)(2\xi+\eta) & -\frac{1}{4}(1+\eta)(\eta-2\xi) & \xi(-1+\eta) & -\frac{1}{2}(1+\eta)(-1+\eta) & -\xi(1+\eta) & \frac{1}{2}(1+\eta)(-1+\eta)\\ -\frac{1}{4}(-1+\xi)(\xi+2\eta) & \frac{1}{4}(1+\xi)(2\eta-\xi) & \frac{1}{4}(1+\xi)(\xi+2\eta) & -\frac{1}{4}(-1+\xi)(2\eta-\xi) & \frac{1}{2}(1+\xi)(-1+\xi) & -\eta(1+\xi) & -\frac{1}{2}(1+\xi)(-1+\xi) & \eta(-1+\xi)\end{bmatrix}$$

$$\times\begin{Bmatrix}x_i & x_j & x_k & x_m & x_n & x_p & x_q & x_r\\ y_i & y_j & y_k & y_m & y_n & y_p & y_q & y_r\end{Bmatrix}^{\mathrm{T}}$$

$\mathbf{J}^{-1}=\frac{1}{det\,\mathbf{J}}\begin{bmatrix}J_1 & J_2\\ J_3 & J_4\end{bmatrix}$ with

$$J_1=-\frac{1}{4}(-1+\xi)(\xi+2\eta)y_i+\frac{1}{4}(1+\xi)(2\eta-\xi)y_j+\frac{1}{4}(1+\xi)(\xi+2\eta)y_k-\frac{1}{4}(-1+\xi)(2\eta-\xi)y_m+$$
$$+\frac{1}{2}(1+\xi)(-1+\xi)y_n-\eta(1+\xi)y_p-\frac{1}{2}(1+\xi)(-1+\xi)y_q+\eta(-1+\xi)y_r$$

$$J_2=\frac{1}{4}(-1+\xi)(\xi+2\eta)x_i-\frac{1}{4}(1+\xi)(2\eta-\xi)x_j-\frac{1}{4}(1+\xi)(\xi+2\eta)x_k+\frac{1}{4}(-1+\xi)(2\eta-\xi)x_m-$$
$$-\frac{1}{2}(1+\xi)(-1+\xi)x_n+\eta(1+\xi)x_p+\frac{1}{2}(1+\xi)(-1+\xi)x_q-\eta(-1+\xi)x_r$$

$$J_3=\frac{1}{4}(-1+\eta)(2\xi+\eta)y_i-\frac{1}{4}(-1+\eta)(\eta-2\xi)y_j-\frac{1}{4}(1+\eta)(2\xi+\eta)y_k+\frac{1}{4}(1+\eta)(\eta-2\xi)y_m-$$
$$-\xi(-1+\eta)y_n+\frac{1}{2}(1+\eta)(-1+\eta)y_p+\xi(1+\eta)y_q-\frac{1}{2}(1+\eta)(-1+\eta)y_r$$

$$J_4=-\frac{1}{4}(-1+\eta)(2\xi+\eta)x_i+\frac{1}{4}(-1+\eta)(\eta-2\xi)x_j+\frac{1}{4}(1+\eta)(2\xi+\eta)x_k-\frac{1}{4}(1+\eta)(\eta-2\xi)x_m+$$
$$+\xi(-1+\eta)x_n-\frac{1}{2}(1+\eta)(-1+\eta)x_p-\xi(1+\eta)x_q+\frac{1}{2}(1+\eta)(-1+\eta)x_r$$

The derivatives of the geometric interpolation functions can be expressed as

$$\frac{\partial\phi_i}{\partial L_i}=1+2L_iL_j+2L_iL_k+2L_iL_m+2L_iL_n+2L_iL_p+2L_iL_q+2L_iL_r-L_j^2-L_k^2-L_m^2-L_n^2-L_p^2-L_q^2-L_r^2$$

$$\frac{\partial\phi_i}{\partial L_j}=L_i^2-2L_iL_j\ ;\ \frac{\partial\phi_i}{\partial L_k}=L_i^2-2L_iL_k\ ;\ \frac{\partial\phi_i}{\partial L_m}=L_i^2-2L_iL_m\ ;\ \frac{\partial\phi_i}{\partial L_n}=L_i^2-2L_iL_n\ ;\ \frac{\partial\phi_i}{\partial L_p}=L_i^2-2L_iL_p\ ;\ \frac{\partial\phi_i}{\partial L_q}=L_i^2-2L_iL_q\ ;\ \frac{\partial\phi_i}{\partial L_r}=L_i^2-2L_iL_r$$

$$\frac{\partial\phi_{ix}}{\partial L_i}=-(x_i-x_j)(2L_iL_j+0.5L_jL_k+0.5L_jL_m+0.5L_jL_n+0.5L_jL_p+0.5L_jL_q+0.5L_jL_r)-(x_i-x_k)(2L_iL_k+0.5L_kL_j+0.5L_kL_m+0.5L_kL_n+0.5L_kL_p+0.5L_kL_q+0.5L_kL_r)-$$
$$-(x_i-x_m)(2L_iL_m+0.5L_mL_j+0.5L_mL_k+0.5L_mL_n+0.5L_mL_p+0.5L_mL_q+0.5L_mL_r)-(x_i-x_n)(2L_iL_n+0.5L_nL_j+0.5L_nL_k+0.5L_nL_m+0.5L_nL_p+0.5L_nL_q+0.5L_nL_r)-$$
$$-(x_i-x_p)(2L_iL_p+0.5L_pL_j+0.5L_pL_k+0.5L_pL_m+0.5L_pL_n+0.5L_pL_q+0.5L_pL_r)-(x_i-x_q)(2L_iL_q+0.5L_qL_j+0.5L_qL_k+0.5L_qL_m+0.5L_qL_n+0.5L_qL_p+0.5L_qL_r)-$$
$$-(x_i-x_r)(2L_iL_r+0.5L_rL_j+0.5L_rL_k+0.5L_rL_m+0.5L_rL_n+0.5L_rL_p+0.5L_rL_q)$$

$$\frac{\partial\phi_{ix}}{\partial L_j}=-(x_i-x_j)(L_i^2+0.5L_iL_k+0.5L_iL_m+0.5L_iL_n+0.5L_iL_p+0.5L_iL_q+0.5L_iL_r)-(x_i-x_k)(0.5L_iL_k)-(x_i-x_m)(0.5L_iL_m)-$$
$$-(x_i-x_n)(0.5L_iL_n)-(x_i-x_p)(0.5L_iL_p)-(x_i-x_q)(0.5L_iL_q)-(x_i-x_r)(0.5L_iL_r)$$

$$\frac{\partial \phi_{ix}}{\partial L_k} = -\left(x_i - x_j\right)\left(0.5L_iL_j\right) - \left(x_i - x_k\right)\left(L_i^2 + 0.5L_iL_j + 0.5L_iL_m + 0.5L_iL_n + 0.5L_iL_p + 0.5L_iL_q + 0.5L_iL_r\right) - \left(x_i - x_m\right)\left(0.5L_iL_m\right) -$$
$$-\left(x_i - x_n\right)\left(0.5L_iL_n\right) - \left(x_i - x_p\right)\left(0.5L_iL_p\right) - \left(x_i - x_q\right)\left(0.5L_iL_q\right) - \left(x_i - x_r\right)\left(0.5L_iL_r\right)$$

$$\frac{\partial \phi_{ix}}{\partial L_m} = -\left(x_i - x_j\right)\left(0.5L_iL_j\right) - \left(x_i - x_k\right)\left(0.5L_iL_k\right) - \left(x_i - x_m\right)\left(L_i^2 + 0.5L_iL_j + 0.5L_iL_k + 0.5L_iL_n + 0.5L_iL_p + 0.5L_iL_q + 0.5L_iL_r\right) -$$
$$-\left(x_i - x_n\right)\left(0.5L_iL_n\right) - \left(x_i - x_p\right)\left(0.5L_iL_p\right) - \left(x_i - x_q\right)\left(0.5L_iL_q\right) - \left(x_i - x_r\right)\left(0.5L_iL_r\right)$$

$$\frac{\partial \phi_{ix}}{\partial L_n} = -\left(x_i - x_j\right)\left(0.5L_iL_j\right) - \left(x_i - x_k\right)\left(0.5L_iL_k\right) - \left(x_i - x_n\right)\left(L_i^2 + 0.5L_iL_j + 0.5L_iL_k + 0.5L_iL_m + 0.5L_iL_p + 0.5L_iL_q + 0.5L_iL_r\right) -$$
$$-\left(x_i - x_m\right)\left(0.5L_iL_m\right) - \left(x_i - x_p\right)\left(0.5L_iL_p\right) - \left(x_i - x_q\right)\left(0.5L_iL_q\right) - \left(x_i - x_r\right)\left(0.5L_iL_r\right)$$

$$\frac{\partial \phi_{ix}}{\partial L_p} = -\left(x_i - x_j\right)\left(0.5L_iL_j\right) - \left(x_i - x_k\right)\left(0.5L_iL_k\right) - \left(x_i - x_p\right)\left(L_i^2 + 0.5L_iL_j + 0.5L_iL_k + 0.5L_iL_m + 0.5L_iL_n + 0.5L_iL_q + 0.5L_iL_r\right) -$$
$$-\left(x_i - x_m\right)\left(0.5L_iL_m\right) - \left(x_i - x_n\right)\left(0.5L_iL_n\right) - \left(x_i - x_q\right)\left(0.5L_iL_q\right) - \left(x_i - x_r\right)\left(0.5L_iL_r\right)$$

$$\frac{\partial \phi_{ix}}{\partial L_q} = -\left(x_i - x_j\right)\left(0.5L_iL_j\right) - \left(x_i - x_k\right)\left(0.5L_iL_k\right) - \left(x_i - x_q\right)\left(L_i^2 + 0.5L_iL_j + 0.5L_iL_k + 0.5L_iL_m + 0.5L_iL_n + 0.5L_iL_p + 0.5L_iL_r\right) -$$
$$-\left(x_i - x_m\right)\left(0.5L_iL_m\right) - \left(x_i - x_n\right)\left(0.5L_iL_n\right) - \left(x_i - x_p\right)\left(0.5L_iL_p\right) - \left(x_i - x_r\right)\left(0.5L_iL_r\right)$$

$$\frac{\partial \phi_{ix}}{\partial L_r} = -\left(x_i - x_j\right)\left(0.5L_iL_j\right) - \left(x_i - x_k\right)\left(0.5L_iL_k\right) - \left(x_i - x_r\right)\left(L_i^2 + 0.5L_iL_j + 0.5L_iL_k + 0.5L_iL_m + 0.5L_iL_n + 0.5L_iL_p + 0.5L_iL_q\right) -$$
$$-\left(x_i - x_m\right)\left(0.5L_iL_m\right) - \left(x_i - x_n\right)\left(0.5L_iL_n\right) - \left(x_i - x_p\right)\left(0.5L_iL_p\right) - \left(x_i - x_q\right)\left(0.5L_iL_q\right)$$

$$\frac{\partial \phi_{iy}}{\partial L_i} = -\left(y_i - y_j\right)\left(2L_iL_j + 0.5L_jL_k + 0.5L_jL_m + 0.5L_jL_n + 0.5L_jL_p + 0.5L_jL_q + 0.5L_jL_r\right) - \left(y_i - y_k\right)\left(2L_iL_k + 0.5L_kL_j + 0.5L_kL_m + 0.5L_kL_n + 0.5L_kL_p + 0.5L_kL_q + 0.5L_kL_r\right) -$$
$$-\left(y_i - y_m\right)\left(2L_iL_m + 0.5L_mL_j + 0.5L_mL_k + 0.5L_mL_n + 0.5L_mL_p + 0.5L_mL_q + 0.5L_mL_r\right) - \left(y_i - y_n\right)\left(2L_iL_n + 0.5L_nL_j + 0.5L_nL_k + 0.5L_nL_m + 0.5L_nL_p + 0.5L_nL_q + 0.5L_nL_r\right) -$$
$$-\left(y_i - y_p\right)\left(2L_iL_p + 0.5L_pL_j + 0.5L_pL_k + 0.5L_pL_m + 0.5L_pL_n + 0.5L_pL_q + 0.5L_pL_r\right) - \left(y_i - y_q\right)\left(2L_iL_q + 0.5L_qL_j + 0.5L_qL_k + 0.5L_qL_m + 0.5L_qL_n + 0.5L_qL_p + 0.5L_qL_r\right) -$$
$$-\left(y_i - y_r\right)\left(2L_iL_r + 0.5L_rL_j + 0.5L_rL_k + 0.5L_rL_m + 0.5L_rL_n + 0.5L_rL_p + 0.5L_rL_q\right)$$

$$\frac{\partial \phi_{iy}}{\partial L_j} = -\left(y_i - y_j\right)\left(L_i^2 + 0.5L_iL_k + 0.5L_iL_m + 0.5L_iL_n + 0.5L_iL_p + 0.5L_iL_q + 0.5L_iL_r\right) - \left(y_i - y_k\right)\left(0.5L_iL_k\right) - \left(y_i - y_m\right)\left(0.5L_iL_m\right) -$$
$$-\left(y_i - y_n\right)\left(0.5L_iL_n\right) - \left(y_i - y_p\right)\left(0.5L_iL_p\right) - \left(y_i - y_q\right)\left(0.5L_iL_q\right) - \left(y_i - y_r\right)\left(0.5L_iL_r\right)$$

$$\frac{\partial \phi_{iy}}{\partial L_k} = -\left(y_i - y_j\right)\left(0.5L_iL_j\right) - \left(y_i - y_k\right)\left(L_i^2 + 0.5L_iL_j + 0.5L_iL_m + 0.5L_iL_n + 0.5L_iL_p + 0.5L_iL_q + 0.5L_iL_r\right) - \left(y_i - y_m\right)\left(0.5L_iL_m\right) -$$
$$-\left(y_i - y_n\right)\left(0.5L_iL_n\right) - \left(y_i - y_p\right)\left(0.5L_iL_p\right) - \left(y_i - y_q\right)\left(0.5L_iL_q\right) - \left(y_i - y_r\right)\left(0.5L_iL_r\right)$$

$$\frac{\partial \phi_{iy}}{\partial L_m} = -\left(y_i - y_j\right)\left(0.5L_iL_j\right) - \left(y_i - y_k\right)\left(0.5L_iL_k\right) - \left(y_i - y_m\right)\left(L_i^2 + 0.5L_iL_j + 0.5L_iL_k + 0.5L_iL_n + 0.5L_iL_p + 0.5L_iL_q + 0.5L_iL_r\right) -$$
$$-\left(y_i - y_n\right)\left(0.5L_iL_n\right) - \left(y_i - y_p\right)\left(0.5L_iL_p\right) - \left(y_i - y_q\right)\left(0.5L_iL_q\right) - \left(y_i - y_r\right)\left(0.5L_iL_r\right)$$

$$\frac{\partial \phi_{iy}}{\partial L_n} = -\left(y_i - y_j\right)\left(0.5L_iL_j\right) - \left(y_i - y_k\right)\left(0.5L_iL_k\right) - \left(y_i - y_n\right)\left(L_i^2 + 0.5L_iL_j + 0.5L_iL_k + 0.5L_iL_m + 0.5L_iL_p + 0.5L_iL_q + 0.5L_iL_r\right) -$$
$$-\left(y_i - y_m\right)\left(0.5L_iL_m\right) - \left(y_i - y_p\right)\left(0.5L_iL_p\right) - \left(y_i - y_q\right)\left(0.5L_iL_q\right) - \left(y_i - y_r\right)\left(0.5L_iL_r\right)$$

$$\frac{\partial \phi_{iy}}{\partial L_p} = -\left(y_i - y_j\right)\left(0.5L_iL_j\right) - \left(y_i - y_k\right)\left(0.5L_iL_k\right) - \left(y_i - y_p\right)\left(L_i^2 + 0.5L_iL_j + 0.5L_iL_k + 0.5L_iL_m + 0.5L_iL_n + 0.5L_iL_q + 0.5L_iL_r\right) -$$
$$-\left(y_i - y_m\right)\left(0.5L_iL_m\right) - \left(y_i - y_n\right)\left(0.5L_iL_n\right) - \left(y_i - y_q\right)\left(0.5L_iL_q\right) - \left(y_i - y_r\right)\left(0.5L_iL_r\right)$$

$$\frac{\partial \phi_{iy}}{\partial L_q} = -\left(y_i - y_j\right)\left(0.5L_iL_j\right) - \left(y_i - y_k\right)\left(0.5L_iL_k\right) - \left(y_i - y_q\right)\left(L_i^2 + 0.5L_iL_j + 0.5L_iL_k + 0.5L_iL_m + 0.5L_iL_n + 0.5L_iL_p + 0.5L_iL_r\right) -$$
$$-\left(y_i - y_m\right)\left(0.5L_iL_m\right) - \left(y_i - y_n\right)\left(0.5L_iL_n\right) - \left(y_i - y_p\right)\left(0.5L_iL_p\right) - \left(y_i - y_r\right)\left(0.5L_iL_r\right)$$

$$\frac{\partial \phi_{iy}}{\partial L_r} = -\left(y_i - y_j\right)\left(0.5L_iL_j\right) - \left(y_i - y_k\right)\left(0.5L_iL_k\right) - \left(y_i - y_r\right)\left(L_i^2 + 0.5L_iL_j + 0.5L_iL_k + 0.5L_iL_m + 0.5L_iL_n + 0.5L_iL_p + 0.5L_iL_q\right) -$$
$$-\left(y_i - y_m\right)\left(0.5L_iL_m\right) - \left(y_i - y_n\right)\left(0.5L_iL_n\right) - \left(y_i - y_p\right)\left(0.5L_iL_p\right) - \left(y_i - y_q\right)\left(0.5L_iL_q\right)$$

Now, we prove the condition: $\phi_i(x_l) = \delta_{il}$. When $l \equiv i$, then r = -1; s = -1 and $L_i = 1$, $L_j = L_k = L_m = L_n = L_p = L_q = L_r = 0$, substituting them into above equations we obtain $\phi_i(x_i) = 1$. Similarly, when $l \equiv j$; $l \equiv k$; $l \equiv m$; $l \equiv n$; $l \equiv p$; $l \equiv q$ or $l \equiv r$, we respectively obtain $\phi_i(x_j) = 0$; $\phi_i(x_k) = 0$; $\phi_i(x_m) = 0$; $\phi_i(x_n) = 0$; $\phi_i(x_p) = 0$; $\phi_i(x_q) = 0$ and $\phi_i(x_r) = 0$.

Next, we prove the conditions: $\phi_{i,x}(x_l) = 0$ and $\phi_{i,y}(x_l) = 0$. When $l \equiv i$, then r = -1; s = -1 and $L_i = 1$, $L_j = L_k = L_m = L_n = L_p = L_q = L_r = 0$, substituting them into above equations we have

$$\begin{Bmatrix} \dfrac{\partial}{\partial\xi} \\ \dfrac{\partial}{\partial\eta} \end{Bmatrix}\begin{bmatrix} L_i & L_j & L_k & L_m & L_n & L_p & L_q & L_r \end{bmatrix} = \begin{bmatrix} -\dfrac{3}{2} & -\dfrac{1}{2} & 0 & 0 & 2 & 0 & 0 & 0 \\ -\dfrac{3}{2} & 0 & 0 & -\dfrac{1}{2} & 0 & 0 & 0 & 2 \end{bmatrix} \quad \Rightarrow \quad \mathbf{J}^{-1} = \frac{1}{det\,\mathbf{J}}\begin{bmatrix} -\dfrac{3}{2}y_i - \dfrac{1}{2}y_m + 2y_r & \dfrac{3}{2}x_i + \dfrac{1}{2}x_m - 2x_r \\ \dfrac{3}{2}y_i + \dfrac{1}{2}y_j - 2y_n & -\dfrac{3}{2}x_i - \dfrac{1}{2}x_j + 2x_n \end{bmatrix}$$

$$\begin{Bmatrix} \dfrac{\partial}{\partial x} \\ \dfrac{\partial}{\partial y} \end{Bmatrix}\begin{bmatrix} L_i & L_j & L_k & L_m & L_n & L_p & L_q & L_r \end{bmatrix} = \mathbf{J}^{-1}\begin{Bmatrix} \dfrac{\partial}{\partial\xi} \\ \dfrac{\partial}{\partial\eta} \end{Bmatrix}\begin{bmatrix} L_i & L_j & L_k & L_m & L_n & L_p & L_q & L_r \end{bmatrix} =$$

$$= \frac{1}{det\,\mathbf{J}}\begin{bmatrix} -\dfrac{3}{2}y_i - \dfrac{1}{2}y_m + 2y_r & \dfrac{3}{2}x_i + \dfrac{1}{2}x_m - 2x_r \\ \dfrac{3}{2}y_i + \dfrac{1}{2}y_j - 2y_n & -\dfrac{3}{2}x_i - \dfrac{1}{2}x_j + 2x_n \end{bmatrix}\begin{bmatrix} -\dfrac{3}{2} & -\dfrac{1}{2} & 0 & 0 & 2 & 0 & 0 & 0 \\ -\dfrac{3}{2} & 0 & 0 & -\dfrac{1}{2} & 0 & 0 & 0 & 2 \end{bmatrix} =$$

$$= \frac{1}{det\,\mathbf{J}}\begin{bmatrix} \dfrac{9}{4}y_i + \dfrac{3}{4}y_m - 3y_r - \dfrac{9}{4}x_i - \dfrac{3}{4}x_m + 3x_r & \dfrac{3}{4}y_i + \dfrac{1}{4}y_m - y_r & 0 & -\dfrac{3}{4}x_i - \dfrac{1}{4}x_m + x_r & -3y_i - y_m + 4y_r & 0 & 0 & 3x_i + x_m - 4x_r \\ -\dfrac{9}{4}y_i - \dfrac{3}{4}y_j + 3y_n + \dfrac{9}{4}x_i + \dfrac{3}{4}x_j - 3x_n & -\dfrac{3}{4}y_i - \dfrac{1}{4}y_j + y_n & 0 & \dfrac{3}{4}x_i + \dfrac{1}{4}x_j - x_n & 3y_i + y_j - 4y_n & 0 & 0 & -3x_i - x_j + 4x_n \end{bmatrix}$$

And $\dfrac{\partial\phi}{\partial L_i} = \dfrac{\partial\phi}{\partial L_j} = \dfrac{\partial\phi}{\partial L_k} = \dfrac{\partial\phi}{\partial L_m} = \dfrac{\partial\phi}{\partial L_n} = \dfrac{\partial\phi}{\partial L_p} = \dfrac{\partial\phi}{\partial L_q} = \dfrac{\partial\phi}{\partial L_r} = 1$. Then, we finally obtain $\phi_{i,x}(x_l) = 0$, $\phi_{i,y}(x_l) = 0$ as

$$\phi_{i,x}(x_i) = \frac{\partial\phi_i}{\partial x} = \begin{bmatrix} \dfrac{\partial\phi_i}{\partial L_i} & \dfrac{\partial\phi_i}{\partial L_j} & \dfrac{\partial\phi_i}{\partial L_k} & \dfrac{\partial\phi_i}{\partial L_m} & \dfrac{\partial\phi_i}{\partial L_n} & \dfrac{\partial\phi_i}{\partial L_p} & \dfrac{\partial\phi_i}{\partial L_q} & \dfrac{\partial\phi_i}{\partial L_r} \end{bmatrix}\begin{Bmatrix} \dfrac{\partial L_i}{\partial x} \\ \dfrac{\partial L_j}{\partial x} \\ \dfrac{\partial L_k}{\partial x} \\ \dfrac{\partial L_m}{\partial x} \\ \dfrac{\partial L_n}{\partial x} \\ \dfrac{\partial L_p}{\partial x} \\ \dfrac{\partial L_q}{\partial x} \\ \dfrac{\partial L_r}{\partial x} \end{Bmatrix} = \begin{bmatrix} 1 & 1 & 1 & 1 & 1 & 1 & 1 & 1 \end{bmatrix}\frac{1}{det\,\mathbf{J}}\begin{Bmatrix} \dfrac{9}{4}y_i + \dfrac{3}{4}y_m - 3y_r - \dfrac{9}{4}x_i - \dfrac{3}{4}x_m + 3x_r \\ \dfrac{3}{4}y_i + \dfrac{1}{4}y_m - y_r \\ 0 \\ -\dfrac{3}{4}x_i - \dfrac{1}{4}x_m + x_r \\ -3y_i - y_m + 4y_r \\ 0 \\ 0 \\ 3x_i + x_m - 4x_r \end{Bmatrix} = 0$$

$$\phi_{i,y}(x_i) = \frac{\partial\phi_i}{\partial y} = \begin{bmatrix} \dfrac{\partial\phi_i}{\partial L_i} & \dfrac{\partial\phi_i}{\partial L_j} & \dfrac{\partial\phi_i}{\partial L_k} & \dfrac{\partial\phi_i}{\partial L_m} & \dfrac{\partial\phi_i}{\partial L_n} & \dfrac{\partial\phi_i}{\partial L_p} & \dfrac{\partial\phi_i}{\partial L_q} & \dfrac{\partial\phi_i}{\partial L_r} \end{bmatrix}\begin{Bmatrix} \dfrac{\partial L_i}{\partial y} \\ \dfrac{\partial L_j}{\partial y} \\ \dfrac{\partial L_k}{\partial y} \\ \dfrac{\partial L_m}{\partial y} \\ \dfrac{\partial L_n}{\partial y} \\ \dfrac{\partial L_p}{\partial y} \\ \dfrac{\partial L_q}{\partial y} \\ \dfrac{\partial L_r}{\partial y} \end{Bmatrix} = \begin{bmatrix} 1 & 1 & 1 & 1 & 1 & 1 & 1 & 1 \end{bmatrix}\frac{1}{det\,\mathbf{J}}\begin{Bmatrix} -\dfrac{9}{4}y_i - \dfrac{3}{4}y_j + 3y_n + \dfrac{9}{4}x_i + \dfrac{3}{4}x_j - 3x_n \\ -\dfrac{3}{4}y_i - \dfrac{1}{4}y_j + y_n \\ 0 \\ \dfrac{3}{4}x_i + \dfrac{1}{4}x_j - x_n \\ 3y_i + y_j - 4y_n \\ 0 \\ 0 \\ -3x_i - x_j + 4x_n \end{Bmatrix} = 0$$

Similarly, we straightforwardly prove the same for $l \equiv j$; $l \equiv k$; $l \equiv m$; $l \equiv n$; $l \equiv p$; $l \equiv q$ or $l \equiv r$, as well as other conditions.